

# Rotational Machine Fault Detection with Ensemble Empirical Mode Decomposition Based on a Three Orthogonal Channel Sensor

Li Tan

Purdue University North Central

[lizhetan@pnc.edu](mailto:lizhetan@pnc.edu)

Alexander Mussa

Purdue University North Central

Justin Poling

Purdue University North Central

Kai Justice

Purdue University North Central

Hongbo Xu

Nanjing University of Science and Technology

## Abstract

Rotational machine fault detection and conditional monitoring can prevent harmful environments and ensure reliable operations of equipment. In order to achieve fault detection and conditional monitoring, many signal processing techniques, such as short-time Fourier transform (STFT), wavelet transform and empirical mode decomposition (EMD), have been developed. Among these methods, the EMD process has been a very promising and effective technique. This paper proposes an EMD-based algorithm that consists of two stages. The first stage processes vibrational signals using three orthogonal channel recordings to obtain a principal component signal. At the second stage, the ensemble empirical mode decomposition (EEMD) is applied to the principal component signal to obtain the intrinsic mode functions (IMF). The Hilbert-Huang transform spectrum based on IMFs for various operating load conditions is examined for fault diagnosis. The proposed algorithm alleviates the computational load by using the principal component signal instead of three individual x-, y-, and z-channel recordings. The experimental validations of the proposed algorithm are demonstrated using vibration signals acquired from a three-phase electric induction motor for healthy and fault conditions under various loads.

## Introduction

For past decades, time-frequency and time-scale analysis methods such as short-time Fourier transform (STFT) and wavelet transform [1-3] have been investigated for analysis of non-stationary or nonlinear signals with applications in rotational machine fault detection and health monitoring to prevent harmful environments and ensure reliable operations of equipment. Although these techniques are successfully applied to machine health diagnosis

and fault detection, the results depend on the selection of window type or the use of a base wavelet. Recently, the Hilbert-Huang transform (HHT) [4,5] has been proposed to decompose a signal into a set of intrinsic mode functions (IMF) via the empirical decomposition (EMD) process [6-10]. The EMD is an adaptive approach and is effective to decompose the non-stationary or nonlinear signals (see details below). However, the EMD process suffers from a problem of mode mixing due to signal intermittency [11,12]. The problem may cause the decomposed results vague and inappropriately interpreted. To eliminate the mode mixing problem, the ensemble empirical mode composition (EEMD) algorithm [11, 12] has been proposed. This method essentially processes the original signal with an added white noise sequence into a set of IMFs using the standard EMD repetitively. The ensemble mean of the corresponding IMFs, which are obtained from the standard EMD, is used as the final EEMD decomposed IMF (see details in below). Although the EEMD is effective for removing the mixing mode problem, the computational load is huge due to the ensemble process. Specially, when applying multi-channel signals such as signals from a sensor that provides three-orthogonal channel information, processing each channel data sequence via the EEMD process requires even more computations and hinders practical applications.

This paper first describes the principles of the standard EMD, Hilbert-Huang transform, and EEMD. To reduce the computational load by using the EEMD for multichannel signals, a principal component empirical decomposition (PCEEMD) algorithm is proposed. The PCEEMD process consists of two stages: the first stage constructs the principal component signal based on the data sensed from three-orthogonal channels, and the second stage applies the standard EEMD process to the principal component signal. After obtaining the IMFs in the principal direction, they can be directly employed for rotational machine fault detection by the HHT spectrum, or, as an option, the obtained IMFs can be projected into three orthogonal axes.

## Algorithm Development

### *Principles of EMD, HT Spectrum, and EEMD*

The EMD is an adaptive decomposition approach which is applied to decompose nonlinear and non-stationary signals. The EMD process extracts a set of IMFs from the original signal. Each IMF must meet two conditions [4]: the number of extrema and the number of zero crossings must be either equal or differ at most by one; the mean value of the envelope defined by the local maxima and the envelope defined by the local minima at any point must be zero. The steps of the EMD algorithm [4-6] to decompose a signal  $x(t)$  is described below:

Step 1: Initialize  $r_0(t) = x(t)$  and set  $i = 0$

Step 2: Extract the  $i$ th IMF with the following sifting procedure:

a. Initialize  $h_{i(k-1)}(t) = r_{i-1}(t)$  with  $k = 1$

- b. Find the local maxima and local minima of signal  $h_{i(k-1)}(t)$
- c. Interpolate the local maxima and local minima by cubic splines to construct the upper and lower envelopes of  $h_{i(k-1)}(t)$
- d. Calculate the mean  $m_{i(k-1)}(t)$  of the upper and lower envelopes of  $h_{i(k-1)}(t)$
- e. Calculate  $h_{ik}(t) = h_{i(k-1)}(t) - m_{i(k-1)}(t)$
- f. If the stop criterion for the iteration  $k$  given below is satisfied

$$\sum_{t=0}^T \frac{[h_{i(k-1)}(t) - h_{ik}(t)]^2}{h_{i(k-1)}^2(t)} \leq SD \quad (1)$$

where SD is a predefined value and usually set to 0.1, that is, if equation 1 is satisfied,  $h_{i(k)}(t)$  is an IMF and then set  $c_i(t) = h_{i(k)}(t)$ ; else set  $k = k + 1$  and then go to step (b).

Step 3: Calculate sequence:  $r_{i+1}(t) = r_i(t) - c_i(t)$

Step 4: If  $r_{i+1}(t)$  has at least 2 extrema then set  $i = i + 1$  and go to step 2; else the decomposition is completed and  $r_{i+1}(t)$  is the residual signal. The decomposition results are listed below:

$$\begin{aligned} x(t) - c_1(t) &= r_1(t) \\ r_1(t) - c_2(t) &= r_2(t) \\ &\dots \\ r_{N-1}(t) - c_N(t) &= r_N(t) \end{aligned}$$

By summing them, it follows that

$$x(t) = \sum_{i=1}^N c_i(t) + r_N(t) \quad (2)$$

It can be seen that signal  $x(t)$  is decomposed into  $N$  intrinsic mode functions and a residue signal  $r_N(t)$ . Once signal  $x(t)$  is decomposed to  $N$  IMFs, the Hilbert transform (HT) [4,5] can be applied to each of IMF to obtain instantaneous frequency, that is,

$$y_i(t) = \frac{1}{\pi} \int_{-\infty}^{\infty} \frac{c_i(\tau)}{t - \tau} d\tau \quad (3)$$

The analytical signal  $z_i(t)$ , which is constructed using both IMF  $c_i(t)$  and its HT  $y_i(t)$ , can be expressed as

$$z_i(t) = c_i(t) + jy_i(t) \quad (4)$$

Then the instantaneous envelope of the analytic signal for the  $i$ th IMF is found to be

$$a_i(t) = \sqrt{c_i^2(t) + y_i^2(t)} \quad (5)$$

and the corresponding phase angle can be determined by

$$\theta_i(t) = \tan^{-1} \left( \frac{y_i(t)}{c_i(t)} \right) \quad (6)$$

Notice that instantaneous envelope  $a_i(t)$  indicates the signal energy variation while the phase angle  $\theta_i(t)$  is the instantaneous phase. The instantaneous frequency for the  $i$ th IMF can be found by taking derivative of the phase angle, that is,

$$\omega_i(t) = \frac{d\theta_i(t)}{dt} \quad (7)$$

The Hilbert transform based on the IMF is referred to Hilbert-Huang transform (HHT); and the time-frequency plot of HHT is referred to HHT spectrum. Although the EMD demonstrates the effectiveness in decomposing nonlinear and non-stationary signals, the method has a problem of mode mixing; that is, a single IMF may contain oscillations of dramatically disparate scales, or a component of a similar scale resides in different IMFs due to signal intermittency. The intermittence could cause serious signal aliasing in time-frequency distribution as well as make the physical meaning of the individual IMF unclear.

The noise-assisted data analysis [11, 12] by adding noise to the original signal is proposed. This method is referred to the ensemble empirical mode decomposition (EEMD). The principle of the EEMD can simply be described as follows. The EEMD adds white noise to the original signal before applying the EMD. Since the added white noise in background populates the whole time-frequency space uniformly, the signal components at different scales can automatically be projected onto proper scales of the references established by the white noise in the background. Although each trail may produce noisy results, the noise in the results can be cancelled out by using the ensemble mean with a significant number of trials. Hence, each IMF obtained using EEMD is the ensemble mean of trials. The EEMD is then summarized below:

- Step 1: Add a white noise sequence to the original signal (the standard deviation of noise =10~20% of the standard deviation of the original signal).
- Step 2: Decompose the signal with added white noise sequence into IMFs [ $c_{i,m}(t)$  at  $m$ th trial] using EMD.
- Step 3: Repeat Steps 1-2 with different white noise sequences for  $M$  times
- Step 4: Calculate the ensemble mean for each IMF

$$c_i(t) = \frac{1}{M} \sum_{m=1}^M c_{i,m}(t), \quad i = 1, 2, \dots, N \quad (8)$$

Obviously, the EEMD algorithm has a large computational load.

### ***Development of Principal Component EEMD***

In many applications, a sensor [13] acquiring signals may contain multi-components. Figure 1 depicts an accelerometer (single station) consisting of three orthogonal x-, y-, and z-channels. Channels x and y are designated to record accelerations in x and y directions, respectively. Channel z measures vertical acceleration. An incoming signal has angles of  $\alpha$ ,

$\beta$ , and  $\gamma$  relative to x-, y-, and z-axes, respectively. Applying the EEMD algorithm for each channel requires a significant amount of computational load.

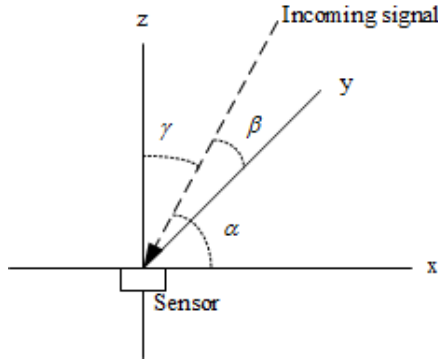


Figure 1. A sensor with x-, y-, z- channel recordings

Assuming  $s(n)$  is the incoming signal with a direction of  $[\cos \alpha \quad \cos \beta \quad \cos \gamma]$  while  $x(n)$ ,  $y(n)$ , and  $z(n)$  are the sensor recordings, the incoming signal can be estimated by a linear combination

$$s(n) = U^T X = [u_1 \quad u_2 \quad u_3] \begin{bmatrix} x(n) \\ y(n) \\ z(n) \end{bmatrix} \quad (9)$$

where  $U^T = [u_1 \quad u_2 \quad u_3]$  and  $X^T = [x(n) \quad y(n) \quad z(n)]$ .

Again, the sensor signals are assumed to be zero mean process, that is,

$$E(X) = \begin{bmatrix} E(x(n)) \\ E(y(n)) \\ E(z(n)) \end{bmatrix} = \begin{bmatrix} 0 \\ 0 \\ 0 \end{bmatrix} \quad (10)$$

then

$$E(s(n)) = E(U^T X) = 0 \quad (11)$$

where  $E(\cdot)$  is the expectation operator. Note that the power of the incoming signal can be expressed as

$$\sigma_s^2 = E(s^2(n)) = U^T E(XX^T)U = U^T CU \quad (12)$$

where  $C$  is a 3x3 covariance matrix defined below:

$$C = E(XX^T) = \begin{bmatrix} \sigma_x^2 & \sigma_{xy} & \sigma_{xz} \\ \sigma_{xy} & \sigma_y^2 & \sigma_{yz} \\ \sigma_{xz} & \sigma_{yz} & \sigma_z^2 \end{bmatrix} \quad (13)$$

with  $\sigma_x^2 = E(x^2(n))$ ,  $\sigma_y^2 = E(y^2(n))$ ,  $\sigma_z^2 = E(z^2(n))$ ,  $\sigma_{xy} = E(x(n)y(n))$ ,

$\sigma_{xz} = E(x(n)z(n))$ , and  $\sigma_{yz} = E(y(n)z(n))$ . Based on Figure 1, it can be seen that

$$X = \begin{bmatrix} x(n) \\ y(n) \\ z(n) \end{bmatrix} = \begin{bmatrix} \cos \alpha \\ \cos \beta \\ \cos \gamma \end{bmatrix} s(n) \quad (14)$$

If  $U^T = [\cos \alpha \quad \cos \beta \quad \cos \gamma]$  is found, the estimated incoming signal becomes

$$s(n) = U^T X = (\cos^2 \alpha + \cos^2 \beta + \cos^2 \gamma) s(n) = 1 \cdot s(n) \quad (15)$$

Equation 15 indicates that  $U^T = [u_1 \quad u_2 \quad u_3]$  should be a unitary vector, that is,  $U^T U = 1$  and the best unitary vector is the one to maximize the power of the incoming signal with the following constraint:

$$\max_{U, \lambda} \sigma_s^2 \quad (16)$$

$$\sigma_s^2 = U^T C U - \lambda^L (U^T U - 1) \quad (17)$$

Taking derivative of  $\sigma_s^2$  to  $U$  and setting the result to zero, it follows that

$$(C - \lambda^L I)U = 0 \quad (18)$$

Taking derivative of  $\sigma_s^2$  to the Lagrange multiplier  $\lambda^L$  and setting the result to zero, the unitary vector constraint  $U^T U = 1$  is yielded. It is clear that the Lagrange multiplier  $\lambda^L$  is essentially an eigenvalue of covariance matrix  $C$ , that is,  $\lambda^L \in \lambda_1^C, \lambda_2^C, \lambda_3^C$ . To ensure  $\sigma_s^2$  to be the maximum value, taking second-order derivative of  $\sigma_s^2$  to  $U$  leads to the following matrix:

$$\frac{\partial^2 \sigma_s^2}{\partial U^2} = \frac{\partial (C - \lambda^L I)U}{\partial U} = C - \lambda^L I = H \quad (19)$$

and  $H$  must be semi-negative definite. Let  $\lambda^H$  and  $U^H$  an eigenvalue and an eigenvector of matrix  $H$ . Equation 19) becomes

$$(H - \lambda^H I)U_H = [C - (\lambda^L + \lambda^H)I]U_H = 0 \quad (20)$$

Equation 20 indicates that  $\lambda^L + \lambda_i^H$  is an eigenvalue of matrix  $C$ , that is,

$$\lambda_i^C = \lambda^L + \lambda_i^H \quad i=1,2,3 \quad (21)$$

and  $U_H = U$ . The eigenvalue of matrix  $H$  can be determined as

$$\lambda_i^H = \lambda_i^C - \lambda^L, \quad i=1,2,3 \quad (22)$$

To ensure  $\lambda_i^H \leq 0$  ( $H$  must be semi-negative definite),  $\lambda^L = \lambda_{\max}^C$ . The corresponding unitary vector  $U$  for  $\lambda_{\max}^C$  is the optimal vector which represents the signal principal direction. With the obtained optimal unitary vector of  $U$ , the principal component signal is achieved as  $s(n) = U^T X$ . Therefore, the proposed principal component ensemble empirical mode decomposition (PCEEMD) algorithm is summarized below:

Step 1: Compute covariance matrix  $C$ .

Step 2: Determine the maximum eigenvalue  $\lambda_{\max}^c$  and its corresponding unitary eigenvector  $U$ .

Step 3: Compute the principal component signal  $s(n) = U^T X$ .

Step 4: Apply the EEMD algorithm to the principal component signal  $s(n) = U^T X$  to obtain IMFs.

Step 5: (optional) Project IMFs to x-, y-, and z-axes, respectively, that is,  $IMFx_i = u_1 \times IMF_i$ ,  $IMFy_i = u_2 \times IMF_i$ ,  $IMFz_i = u_3 \times IMF_i$

## Experiments and Validations

To validate the proposed PCEEMD method for non-stationary or nonlinear signal analysis, vibrational signals from the accelerometer based on three-orthogonal channels were acquired from the three-phase induction motor with an adjustable load (Figure 2). As shown in Figure 2, an accelerometer was attached on the three-phase induction motor. The accelerations measured in x-, y-, z- axes were obtained via LabView data acquisition platform at a sampling rate of 10 kHz with a 16-bit data resolution. The acquired data sequence from each channel was preprocessed to remove its mean (DC component). The adjustable load via the belt was coupled to the motor via a rubber coupler. A fault in the rubber coupler was introduced. Figure 3 shows healthy and fault coupler conditions. The coupler in fault condition has inner and outer worn-out teeth on the driving side. The experiments were carried out with no load (0% load), medium load (50% load), and full load (100% load) with the motor running at 1,800 rpm. The speed of the shaft was monitored by an optical encoder.

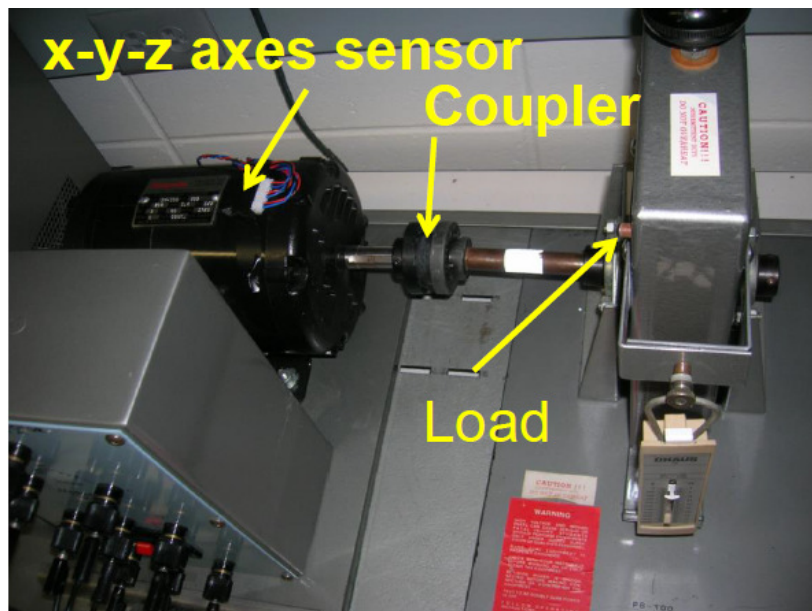


Figure 2. Experimental setup

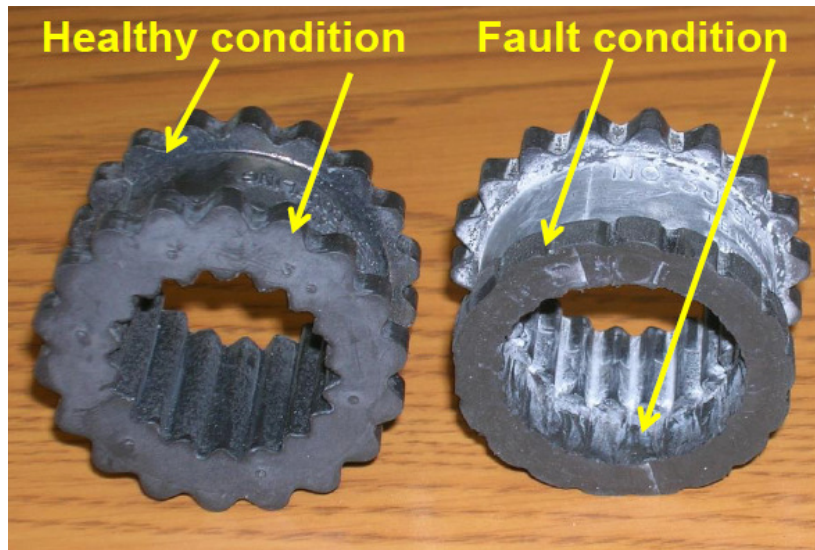


Figure 3. Coupler healthy condition and fault condition

Notice that for the healthy condition validation experiment, the healthy coupler was installed while for the fault condition validation, the healthy coupler was simply replaced by the fault coupler. It is also assumed that the condition for the healthy coupler or the fault coupler stays the same during testing. The transition condition between the healthy coupler and fault coupler is not considered in this paper and will be investigated in the future.

Figure 4 shows x-y-z channel vibration signals measured from the sensor as well as the principal component signal produced by the PCEEMD algorithm for the healthy coupler and fault coupler under the 50% load.

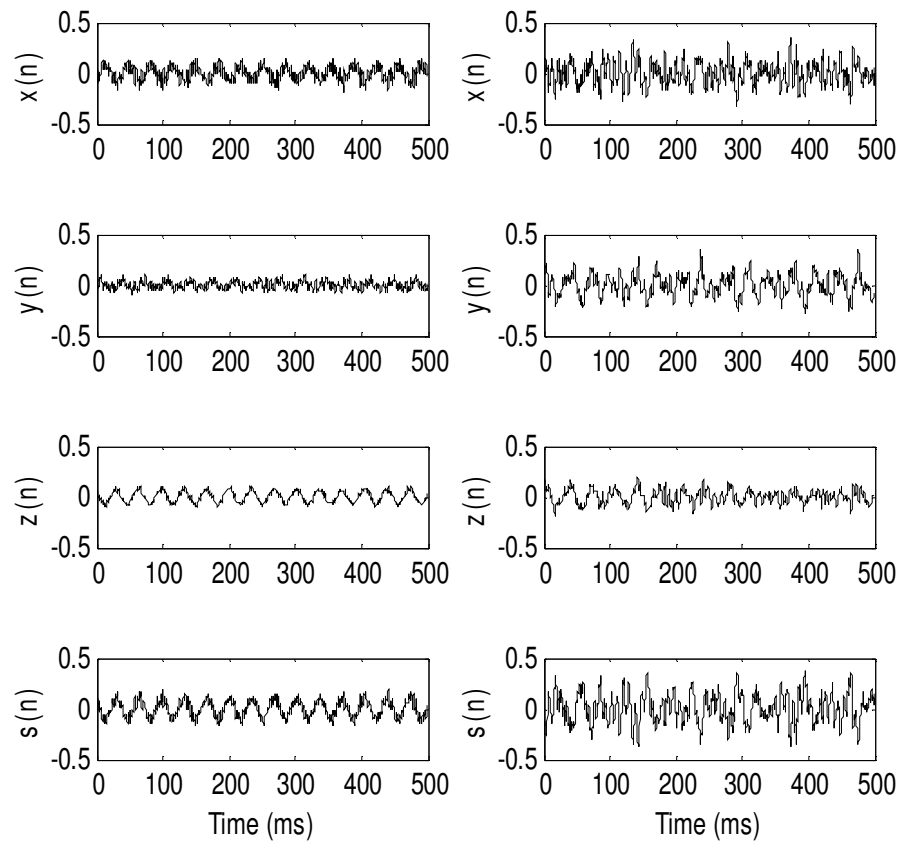


Figure 4. Acceleration measurements and generated principal component signal  $s(n)$   
(left: healthy condition; right: fault condition)

The second stage applied the EEMD algorithm to the principal component signals. The principal component signal was added with a white noise sequence with a Gaussian distribution using 20% of the standard deviation of the original signal. The ensemble mean of each IMF is calculated using 50 trials. The achieved corresponding IMFs for both healthy and fault conditions are given in Figure 5 for comparisons. It can be seen that for both cases, there are no significant evidences of mixing modes. The shaft frequency of 30 rev/s can be seen in IMF6 for both cases. For the healthy condition, there are 9 IMFs but 10 IMFs for the fault

condition.

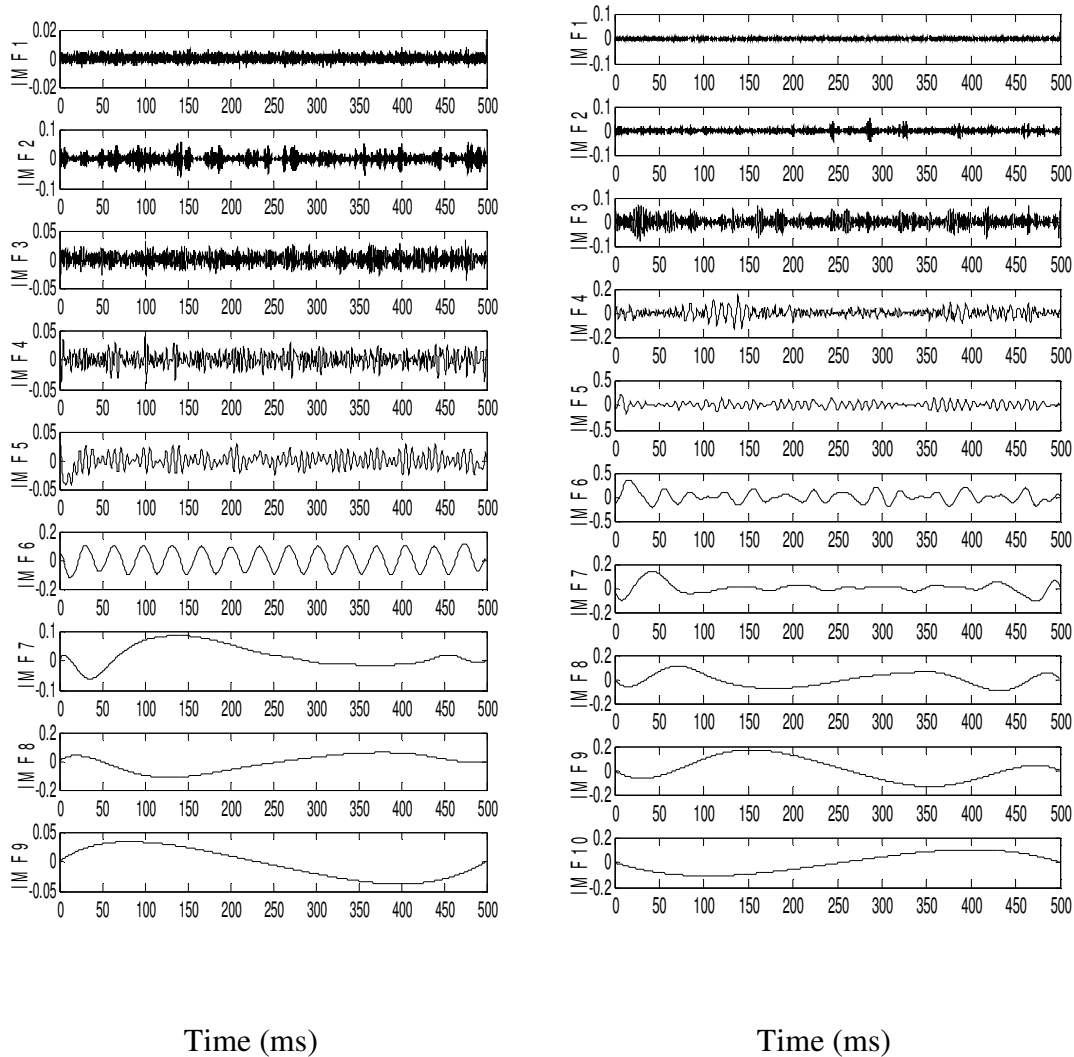


Figure 5. Decomposed IMFs from two coupler conditions using the PCEEMD algorithm (left: healthy condition; right: fault condition)

The corresponding HHT spectra for healthy and fault conditions are depicted in Figure 6. As shown Figure 6a, the dominant frequency component comes from the shaft rotation, that is, 30 Hz (rev/sec); and for the fault condition as shown in Figure 6b, besides the dominant frequency component of the shaft rotation (30 Hz), there appear the fourth harmonic component, irregular pulses and high frequency noise. As an additional validation, the discrete-Fourier transform spectra were calculated and displayed in Figure 7. Clearly, the shaft frequency component is dominant for both healthy and fault conditions. Similarly, the fourth harmonic frequency component becomes significant in the fault condition. However, the DFT spectrum does not show time-scale information.

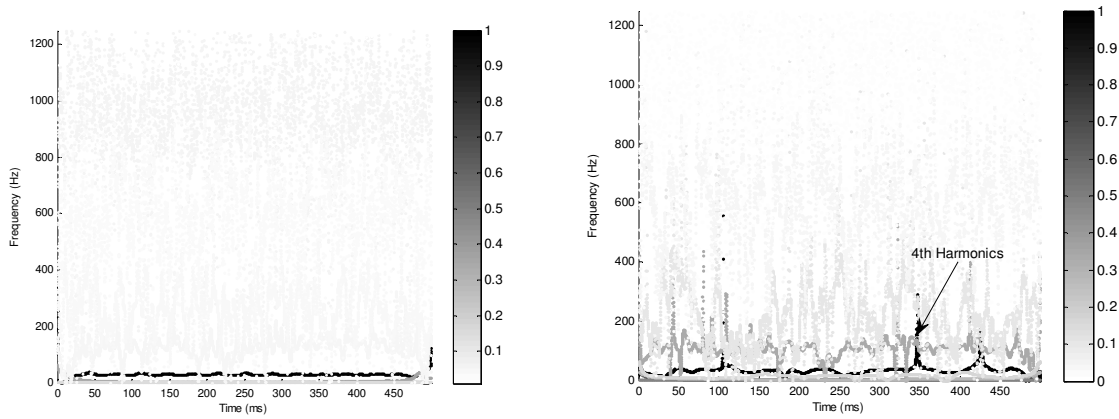


Figure 6. The HHT spectra from two coupler conditions using the PCEEMD algorithm (left: Healthy condition; right: fault condition)

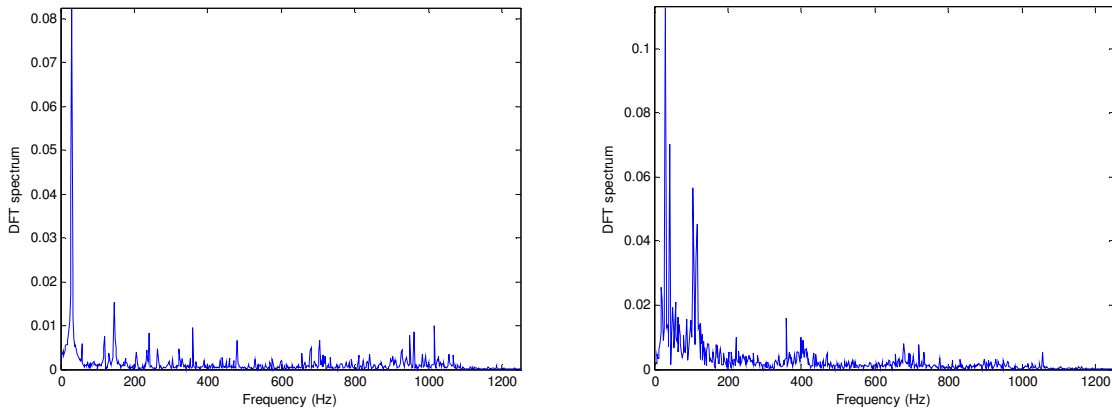


Figure 7. DFT spectra from two coupler conditions using the PCEEMD algorithm (left: healthy condition; right: fault condition)

### Additional Results

The validations for the 0% and 100% loads also show the similar results as that of the 50% load. The results are consistent and summarized in Table 1.

Table 1. Results from HHT Spectra

Operation Conditions	Dominant frequency	High-order harmonics	Irregular pulses	High frequency noise
Healthy, 0% load	Significant	Not Significant	Not Significant	Not Significant
Faulty, 0% load	Significant	Significant	Significant	Significant
Healthy, 50% load	Significant	Not Significant	Not Significant	Not Significant
Faulty, 50% load	Significant	Significant	Significant	Significant
Healthy, 100% load	Significant	Not Significant	Not Significant	Not Significant
Faulty, 100% load	Significant	Significant	Significant	Significant

Since the EEMD process only applies to the principal component signal, the computational load is significantly reduced. Most importantly, since the principal component signal contains the sensed vibration signal with its aligned direction so that the obtained IMFs and HHT spectra will present most meaningful information for fault detection and conditional monitoring.

## Conclusion

This paper proposed a principal component ensemble empirical decomposition (PCEEMD) algorithm for rotational machine fault detection and conditional monitoring. The algorithm is very effective for processing data from a single station sensor with x-, y-, and z- sensing components. The PCEEMD consists of two stages. The first stage performs vibrational signal enhancement to achieve the principal component signal according to three orthogonal channel recordings. With the principal component signal, the EEMD algorithm is applied to obtain the IMFs with an advantage of mixing mode elimination. The Hilbert-Huang transform spectra are then obtained for rotational machine fault detection and diagnosis. The algorithm significantly alleviates the computational load by processing the principal component signal instead of three individual channel recordings. The experimental validations of the proposed method are demonstrated using vibration data acquired from the three-phase electric motor for healthy and fault conditions under various loads.

## References

- [1] Satish, L. (1998). Short-Time Fourier and Wavelet Transform for Fault Detection in Power Transformers during Impulse Test. *Proceedings of the Institute of Electrical Engineering, Science, Measurement and Technology*, 145, 77-84.
- [2] Wang, C., & Gao, R. (2003). Wavelet Transform with Spectral Post-Processing for Enhanced Feature Extraction. *IEEE Transactions on Instrumentation and Measurement*, 52, 1296-1301.
- [3] Tan, L., & Jiang, J. (2013). *Digital Signal Processing: Fundamentals and Applications*. (2nd ed.). Amsterdam: Elsevier.
- [4] Huang, N. E., Zheng, S., & Steven, R. L. (1998). The Empirical Mode Decomposition Method and the Hilbert Spectrum for Non-Stationary Time Series Analysis. *Proceedings of Royal Society of London*, A454, 903-995.
- [5] Feldman, M. (2011). Hilbert Transform in Vibration Analysis. *Mechanical Systems and Signal Processing*, 25, 735-802.
- [6] Lei, Y., Lin, J., He, Z., & Zuo, M. (2013). A Review on Empirical Mode Decomposition in Fault Diagnosis of Rotating Machinery. *Mechanical Systems and Signal Processing*, 35, 108-126.
- [7] Liu, B., Riemenschneider, S., & Xu, Y. (2006). Gearbox Fault Diagnosis Using Empirical Mode Decomposition and Hilbert Spectrum. *Mechanical Systems and Signal Processing*, 20, 718-734.
- [8] Li, R., & He, D. (2012, April). Rotational Machine Health Monitoring and Fault Detection Using EMD-Based Acoustic Emission Feature Quantization. *IEEE Transactions on Instrumentation and Measurement*, 61(4), 990-1001.  
*Proceedings of The 2014 IAJC-ISAM International Conference*  
ISBN 978-1-60643-379-9

- [9] Yang, W., Court, P. J., Tavner, & Crabtree, C. J. (2011). Bivariate Empirical Mode Decomposition and Its Contribution to Wind Turbine Condition Monitoring. *Journal of Sound and Vibration*, 330, 3766-3782.
- [10] Gao, Q., Duan, C., Fan, H., & Meng, Q. (2008). Rotating Machine Fault Diagnosis Using Empirical Mode Decomposition. *Mechanical Systems and Signal Processing*, 22, 1072-1081.
- [11] Zhang, J., Yan, R., Goa, R., & Feng, Z. (2010). Performance Enhancement of Ensemble Empirical Mode Decomposition. *Mechanical System and Signal Processing*, 24, 2104-2123.
- [12] Yan, R., Zhao, R., & Gao, R. (2012, December). Noise-Assisted Data Processing in Measurement Science: Part Two. *IEEE Instrumentation and Measurement Magazine*, 15(6), 32-35.
- [13] Magotra, N., Ahmed, N., & Chael, E. (1989, January). Single-Station Seismic Event Detection and Location. *IEEE Transactions on Geoscience and Remote Sensing*, 27(1), 15-23.

## Biographies

LI TAN is a professor with the College of Engineering and Technology, Purdue University North Central. He received the B.S. degree from the Southeast University, Nanjing, China, in 1984, and the M.S. degree in Structural Engineering and the M.S. and Ph.D. degrees in Electrical Engineering from the University of New Mexico, Albuquerque, in 1987, 1989, and 1992, respectively. Dr. Tan is an IEEE Senior Member since 2001. His research interests include the areas of digital signal processing, active noise control and control systems, and digital communications. He co-authored two textbooks: *Digital Signal Processing: Fundamentals and Applications*, 2nd ed., Elsevier, 2013; and *Analog Signal Processing and Filter Design*, Linus Publications, 2009. He holds a US patent. He has served as an associate editor for the *International Journal of Engineering Research and Innovation*, and *International Journal of Modern Engineering*.

ALEXANDER MUSSA is a senior electrical engineering student at College of Engineering and Technology, Purdue University North Central.

JUSTIN POLING is a senior electrical engineering student at College of Engineering and Technology, Purdue University North Central.

KAI JUSTICE is a senior electrical engineering student at College of Engineering and Technology, Purdue University North Central.

HONGBO XU is a Ph.D. student at the School of Mechanical Engineering, Nanjing University of Science and Technology, Nanjing, China. He is a visiting scholar in spring 2014, at College of Engineering and Technology, Purdue University North Central.